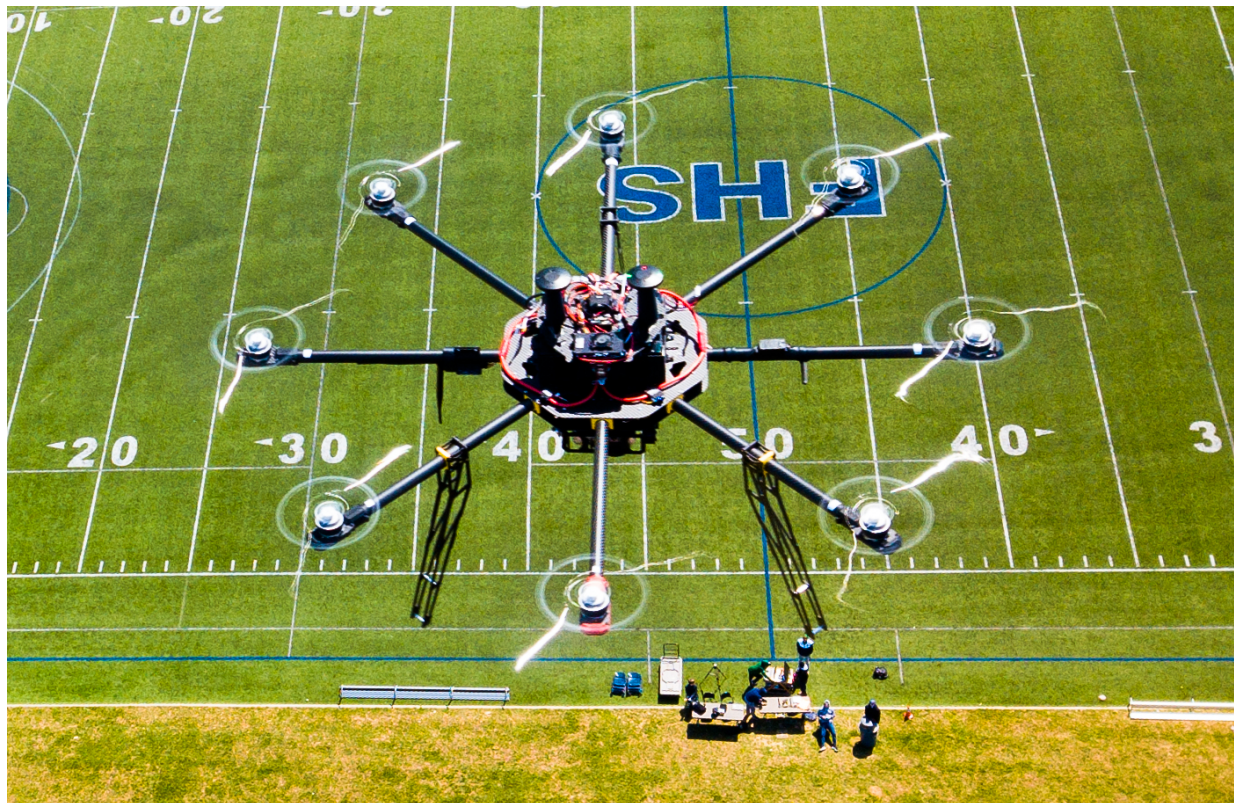


Animus Ferus

2018 AUVSI SUAS



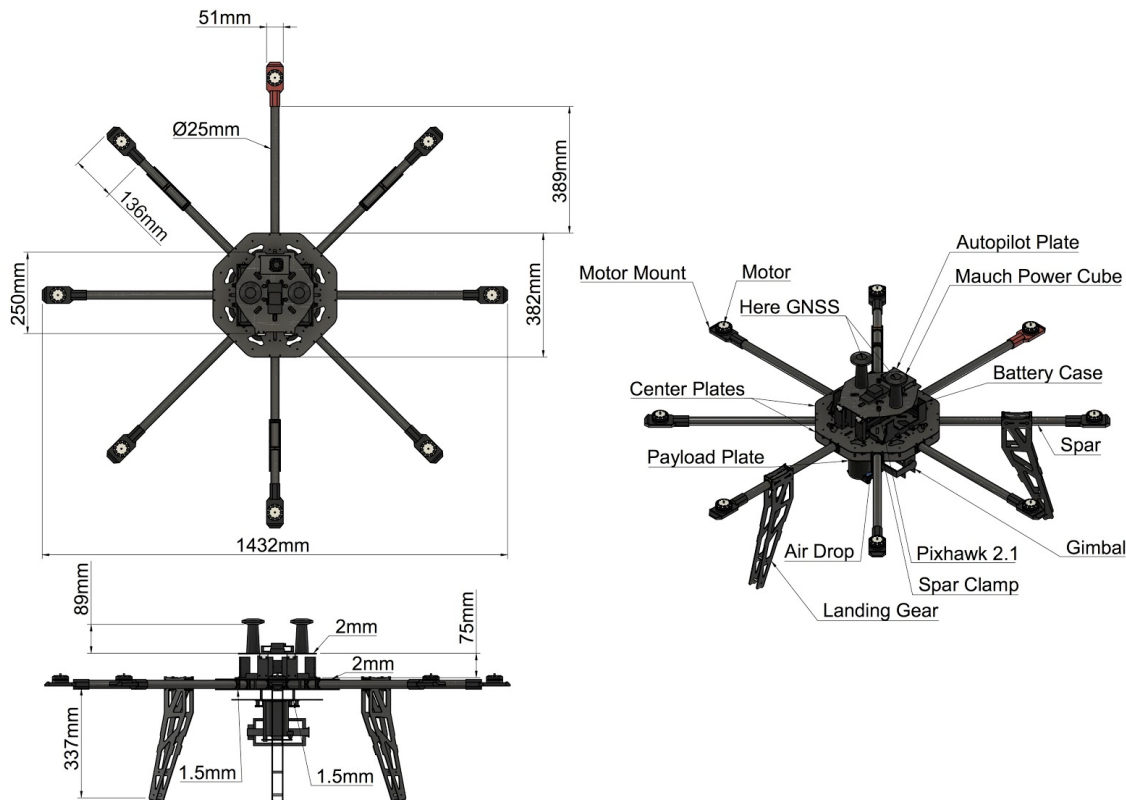
Abstract

Team Animus Ferus built upon past experience with multirotors to engineer a new octocopter for the 2018 AUVSI Student Unmanned Aerial Systems (SUAS) competition. The team's main goal for the 2018 SUAS competition was to develop a reliable Unmanned Aerial System (UAS) that could complete all Mission Demonstration elements. This Technical Design Paper outlines the design of Spirit X, the team's new competition Unmanned Aerial Vehicle (UAV). Spirit X represents a significant milestone for team Animus Ferus: the first fully in-house engineered multirotor UAV. The UAV was designed from the ground up solely by team members and is equipped with a new, higher efficiency propulsion system, a new redundant electrical system, an updated flight controller, a much stronger airframe, and significantly improved software control systems. These new components all contribute to a much improved mission demonstration performance. Additionally, the team improved last year's UAV, Spirit IX, to use as a test platform.

Table of Contents

1. Systems Engineering Approach	3
1.1. Mission Requirement Analysis.....	3
1.2. Design Rationale.....	4
2. System Design	5
2.1. Aircraft.....	5
2.2. Autopilot.....	6
2.3. Obstacle Avoidance.....	7
2.4. Imaging System.....	8
2.5. Object Detection, Classification, Localization (ODCL).....	9
2.5.1 Design.....	9
2.5.2 Manual Target Submission.....	9
2.5.3 Autonomous Target Detection.....	10
2.5.4 Autonomous Color Classification.....	11
2.5.5 Autonomous Shape Classification.....	11
2.5.6 Autonomous Letter and Orientation Classification.....	11
2.5.7 Developmental Testing.....	11
2.6. Communications.....	12
2.7. Air Delivery.....	13
2.8. Cybersecurity.....	14
3. Safety, Risks, and Mitigation	14
3.1. Developmental Risks & Mitigations.....	15
3.2. Mission Risks & Mitigations.....	15
4. Conclusion	15

Figure 1: Spirit X Specifications



1. Systems Engineering Approach

Spirit X was designed to complete the search and rescue mission outlined in the 2018 SUAS competition rules as safely, accurately, and reliably as possible. The UAV is capable of fully autonomous flight, autonomous obstacle avoidance, autonomous image processing, and autonomous payload delivery.

1.1. Mission Requirement Analysis

At the beginning of the development process, team Animus Ferus analyzed the requirements of the 2018 SUAS competition to develop a list of systems Spirit X needed for optimal performance during the mission demonstration. **Table 1** outlines this analysis for each mission demonstration task and the systems that must be developed to successfully accomplish said task.

Table 1: Mission Requirements Analysis

Task	Task Requirements	Requirements for Successful Task Completion
Timeline (10%)	<ul style="list-style-type: none"> Complete the mission in as little flight time and post processing time as possible (80%) Do not take a timeout (20%) 	<ul style="list-style-type: none"> The team must be well prepared for the mission and the UAS must be thoroughly tested to ensure a successful flight Safely complete the mission as quickly as possible
Autonomous Flight (30%)	<ul style="list-style-type: none"> Fly autonomously with minimal manual takeovers (40%) Fly a sequence of waypoints within 100 ft of each waypoint (10%) Capture waypoints with high accuracy (50%) 	<ul style="list-style-type: none"> Waypoints must be captured with high accuracy to maximize points
ODCL (20%)	<ul style="list-style-type: none"> Identify target shape, shape color, alphanumeric, alphanumeric color and orientation (20%) Locate each target and submit its GPS position to the interoperability server (30%) Complete actionable submission of target information (30%) Complete image processing autonomously (20%) 	<ul style="list-style-type: none"> The UAS must implement a communications system capable of transmitting images from the UAV to the Ground Control Station (GCS) Targets must be able to be captured both manually and autonomously, with successful target classification and submission of data to the interoperability server
Obstacle Avoidance (20%)	<ul style="list-style-type: none"> Avoid stationary obstacles (50%) Avoid moving obstacles (50%) 	<ul style="list-style-type: none"> The UAV must navigate around stationary and moving obstacles autonomously
Air Delivery (10%)	<ul style="list-style-type: none"> Accurately deliver the payload (100%) The water bottle must open upon impact to receive any points for drop accuracy 	<ul style="list-style-type: none"> The UAV must have a mechanism that can integrate with the Pixhawk 2.1, be released autonomously, and provide high-precision drops
Operational Excellence (10%)	<ul style="list-style-type: none"> Practice professional behavior through communications and team actions 	<ul style="list-style-type: none"> The team must practice the mission in advance to ensure optimal communication and safety protocols are always implemented

Team Animus Ferus analyzed each mission component to determine the maximum number of points that could be acquired while minimizing the chance of mission failure. During this analysis, *Autonomous Flight* was flagged as the most important mission task to complete, as is shown in **Table 1**. Successfully completing the *Autonomous Flight* task would require implementing a system such as ArduPilot in conjunction with a full suite of sensors to ensure reliability and safety during flight. Next, the team decided that an autonomous *Obstacle Avoidance* algorithm would be beneficial since it would enable GCS operators to focus on other tasks during the mission demonstration. In addition, the *ODCL* task required a high-resolution camera with stabilization. The *Air Delivery* task required an airdrop mechanism capable of autonomous payload delivery with high accuracy. Furthermore, the mechanism chosen must ensure the water bottle will break on impact, which could take place on grass, concrete, pavement, or dirt. Finally, the *Timeline* and *Operational Excellence* tasks required extensive preparation for the mission as well as a reliable UAS.

Addressing these mission tasks required Animus Ferus to develop a new UAV rather than build on Spirit IX, the team's competition UAV for the 2017 SUAS competition. Maximizing reliability, safety, and mission score required the team to make numerous design tradeoffs. For instance, the propulsion system was redesigned to provide significantly increased flight range, but this also increased the UAV's weight. Additionally, the electrical system was redesigned from the ground up to maximize redundancy and efficiency at the cost of higher complexity and greater potential of human error during assembly.

1.2. Design Rationale

Team Animus Ferus is entirely composed of high school students attending Flint Hill School. The team's sole advisor is Michael Snyder, the robotics and computer science teacher at Flint Hill. Several members have had over two years of development with UAVs and are very familiar with multirotor designs. The majority of the development team comprises new members.

In addition to an analysis of the mission requirements for the 2018 SUAS competition, an analysis of Spirit IX's flaws was executed early in the development process. This analysis revealed numerous issues, precluding Spirit IX's use as a base for Spirit X. In particular, the propulsion system did not have acceptable efficiency or enough thrust to support the expanded mission tasks that would be attempted during the 2018 SUAS competition. Additionally, the airframe was not large enough to add new flight components required for improved mission demonstration performance. Further, the flight control system was outdated, the airdrop mechanism was unreliable, and the imaging system's gimbal had multiple software compatibility and technical issues.

Figure 2: Design Flowchart

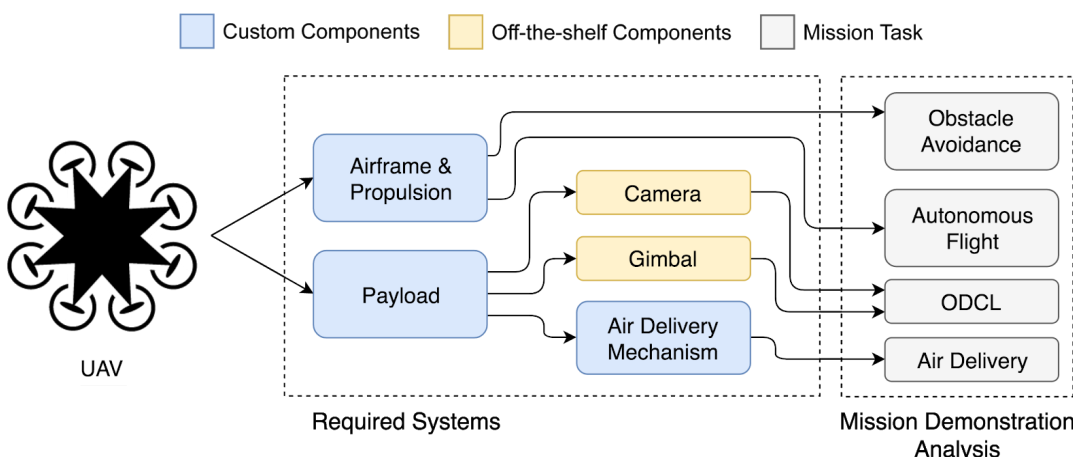


Figure 2 outlines Animus Ferus' design priorities. To address the aforementioned disadvantages of Spirit IX, team Animus Ferus chose to design Spirit X from the ground up. During the design process, the team weighed the benefits of a multirotor versus a fixed wing design. Although fixed wing designs provide greater maximum range, multirotors are also capable of flying at distances that well exceed those required by the SUAS competition.

Multirotor UAVs offer higher stability than similarly-sized fixed wing systems and also provide redundancy in the propulsion system. Multirotor UAVs also offer more precise maneuvering than fixed wing aircraft. In order to maximize flight control, yielding higher point acquisition during waypoint navigation, and in view of significant experience with multirotor craft, the team chose an octocopter. After deciding on the type of UAV to design, the team analyzed each mission component and determined what systems would work optimally for that task.

Once the type of UAV was selected, the most important design decision was the choice of the autopilot system. The autopilot system influenced the airframe choice, imaging subsystem, and air delivery mechanism. Team Animus Ferus chose the Pixhawk 2.1 running ArduPilot with a full sensor suite because of the large support community and extensive capabilities. Paired with Mission Planner as the Ground Control Station, the Pixhawk 2.1 would be capable of completing fully autonomous flight.

No commercial airframes were suitable for Spirit X's requirements, and after an extensive process of deliberation, the team decided to engineer a frame that would enable maximum mission score, reliability, and safety.

For the imaging subsystem, the team chose to use the Samsung NX500 with a new 2-axis gimbal that would provide high quality pictures during flight. Using a gimbal system with the camera ensured that captured images would not contain any motion blur, maximizing the quality of the images taken in the search area.

Animus Ferus designed the air delivery mechanism from PLA+ plastic, adapting it to the specific requirements of Spirit X's airframe and the location of the gimbal and camera. It is controlled through the Pixhawk 2.1's auxiliary outputs, and is placed in a location on the craft that reduced the impact on the UAV's center of mass when the payload is released.

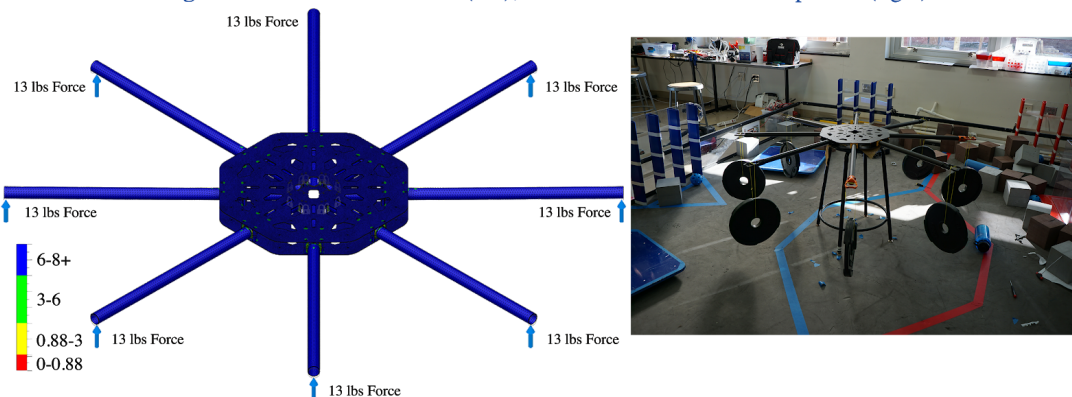
2. System Design

2.1. Aircraft

Animus Ferus designed Spirit X's airframe to offer significant performance improvements over Spirit IX. As previously mentioned, supporting the team's expanded mission goals required a full rebuild of the airframe from the ground up. To minimize the weight of the UAV while maximizing strength, all airframe components were designed and constructed using 3K carbon fiber. The battery case was printed with PLA+ plastic. This plastic is a strong, temperature-resistant 3D printer filament capable of operating in outdoor conditions.

The airframe consists of eight 610mm long by 25mm diameter carbon fiber spars which are mounted between two center plates, with an additional two smaller carbon fiber plates attached to mount the autopilot system and payload. Both center plates measure 382 mm in diameter - with the bottom plate being 1.5 mm thick and the top plate being 2 mm thick. **Figure 1**, found on page 2, provides a rendered visual of Spirit X and contains all relevant craft dimensions.

Figure 3: Simulated Stress Test (left), Airframe Stress Test with 80 pounds (right)



The autopilot and payload plates were designed to be easily taken off and replaced as needed to minimize footprint during travel and to simplify testing. During development, static stress tests were conducted on the airframe. The results from one of the static stress test can be seen in **Figure 3**, which shows that the UAV has a safety factor of 6+ when exposed to 104 lbs of constant force. Further stress tests were conducted on the frame once

it was constructed to determine the maximum safe load. These tests showed that the frame was able to withstand a simulated flight mass of 36.36 kg, far exceeding the UAV's mass of 12.8 kg.

The *Air Delivery* mechanism and the imaging system are mounted to the payload plate, which connects to the bottom of the core section of the UAV. The autopilot plate, shown as the top-most carbon fiber plate in **Figure 1** on page 2, rotates up to allow easy access to the batteries, which are attached via a custom-designed, 3D-printed case made from PLA+ plastic. Neoprene and foam are added as padding around the batteries, dampening vibrations and improving the accuracy of measurements from the Pixhawk 2.1's Inertial Measurement Units (IMU) in-flight. This in turn allows for a stable craft and ensures that the batteries will not shift due to the imposition of external forces. Two MaxAmps 23Ah 6S 25C Li-Po batteries are run in parallel, with each Li-Po battery having its own connection to the power distribution board. Each battery connection is capable of running the octocopter individually, providing redundancy in the event of a battery failure or a wire disconnect. Further, the Pixhawk 2.1 has redundant power systems which are enabled at all times.

Eight each of the KDE 4312XF 360 kV motors, 55A KDE Electronic Speed Controllers (ESC), and 18.5" x 6.3" KDE folding carbon fiber propellers are used as the components for the new propulsion system. During testing, these systems produced over 80 lbs of thrust at maximum throttle, giving Spirit X a Thrust to Weight ratio of 2.93:1, as shown in **Table 2**. The propellers are designed to operate optimally with the chosen motors and ESCs, which provide regenerative braking and a refresh rate of 420 Hz, enabling near-instantaneous flight adjustments. When compared to Spirit IX, the redesigned propulsion system provides Spirit X with a 43% increase in max thrust and a 5% efficiency boost in optimal flight conditions. This efficiency improvement, in conjunction with the improved electrical system, outlined above, translates to an additional flight range of 1.6 km during optimal flight. Further, the new propulsion system minimizes vibration, enabling smooth flight and higher quality image captures in the search area.

As shown in **Table 2**, the redesigned airframe, propulsion system, and electrical subsystem provide Spirit X with the following flight characteristics.

Table 2: Aircraft Properties

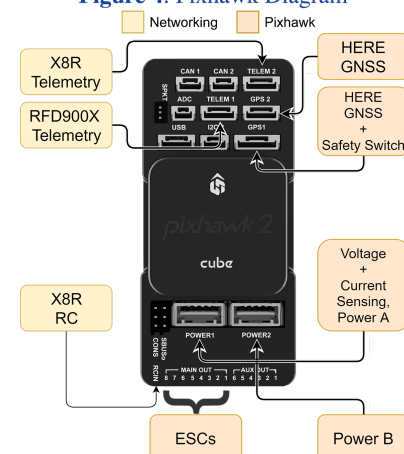
Aircraft Properties					
Max Speed (knots)	30	Thrust to Weight Ratio	2.93:1	Frame Weight (kg)	6.5
Operational Range (km)	2.5	Diameter with Propellers (mm)	1750	Payload (kg)	6.3
Max Flight Range (km)	7.4	Diameter (mm)	1432	Gross Weight (kg)	12.8
Max Flight Time (minutes)	40	Height (mm)	560	Maximum Takeoff Weight (kg)	17.0

2.2. Autopilot

Spirit X uses the Pixhawk 2.1 autopilot, integrated with a full sensor suite for autonomous flight. **Figure 4** shows the wiring of this system and how all individual components are connected. The Pixhawk 2.1 has built-in IMU sensor redundancy, internal vibration dampening, and redundant power supply systems, which increase the safety and reliability of Spirit X. The modularity of the Pixhawk 2.1 supported the Test Driven Development approach Animus Ferus implemented during development. Each autopilot system component was individually unit tested, simulation tested, and then integrated with the Spirit X UAV. This approach enabled the team to identify issues pre-flight and tune the craft for optimal autonomous operation at competition.

To communicate with the Pixhawk 2.1, MavProxy acts as an initial communication hub and duplicates the MAVLink connection to enable the

Figure 4: Pixhawk Diagram



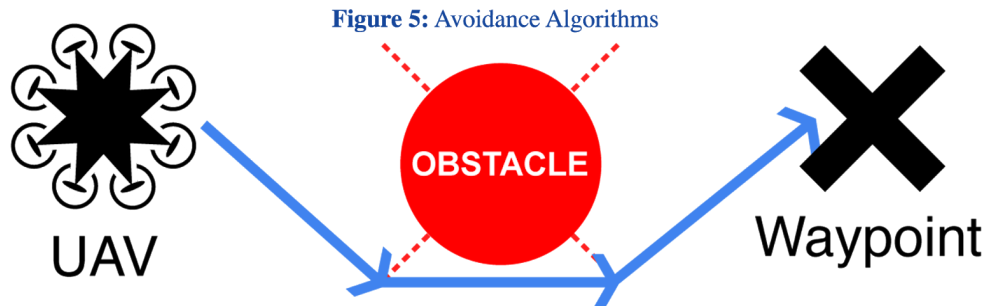
use of multiple control systems: Mission Planner and a custom GCS software stack.

Mission Planner serves as Spirit X's main control hub and enables actionable monitoring of the UAV and all equipment on board while also providing the GCS operator with the ability to execute control operations at any time. Mission Planner's advanced functionality was one of the key reasons it was chosen as the main GCS user interface.

Additionally, two other user interfaces were custom developed, one acting as the interface for the judges to view mission information and the other as an interface to the systems running *Obstacle Avoidance* and *ODCL*. The custom web-based user interface displays the UAV's current position along with all required mission information and is updated multiple times per second, ensuring live data is always displayed to the judges. The other interface enables the team to ensure that data is successfully being communicated to and from the interoperability server. Further, this interface allows the team to start and stop the *Obstacle Avoidance* and *ODCL* systems during flight. This functionality is key because it enables the GCS operator to stop the systems in the event of system failure on the UAV. The interface also enables team members to submit targets manually during post processing time.

2.3. Obstacle Avoidance

To accomplish *Obstacle Avoidance*, Animus Ferus developed a custom suite of algorithms that interact with the UAV to guide it around stationary and moving obstacles. A number of different approaches were considered, including vector-field and A* based pathing systems. These approaches were analyzed to determine their feasibility for use as the Obstacle Avoidance Program (OAP). During this analysis, Animus Ferus identified a number of difficulties with implementing these systems. Specifically, the vector-field approach required extensive testing that would not be completed within the time span allotted for OAP development. The A* algorithm was determined to not be optimal for flight due to the potential for a significant number of flight path changes required to avoid obstacles. Such flight path changes take a heavy toll on multirotor craft and consume a significant amount of power. For these reasons, Animus Ferus chose to design algorithms from scratch to address the *Obstacle Avoidance* mission task.



Spirit X utilizes the OAP to avoid both moving and stationary obstacles. The OAP first checks whether the obstacles are inside the flight zone boundary, and if so, determines if the obstacles intersect with the UAV's current flight path. If an obstacle does intersect, the OAP will efficiently create an avoidance path around the obstacle, minimizing the distance the UAV has to travel to avoid the obstacle, as seen in **Figure 5**. The system is capable of addressing all edge cases including overlapping obstacles and obstacles over the air drop location.

To ensure the validity of the OAP, the team conducted extensive testing of the system. All software algorithms passed extensive unit tests and simulation tests. After successfully testing the OAP on over 2,000 waypoints and 500 simulated obstacles, the system was tested using Spirit IX. Thirteen stationary obstacles and five moving obstacles were tested with Spirit IX. Upon the successful completion of the tests conducted on Spirit IX, the OAP was integrated into Spirit X and then thoroughly tested once again. **Table 3** summarizes the results from the tests conducted with the OAP in the final competition configuration of Spirit X.

Table 3: SDA Testing Information

	Number of Obstacles Tested	Successfully Avoided	Percent Successful Avoidance
Stationary Obstacles	16	13	81%
Moving Obstacles	4	2	50%

The OAP is extremely lightweight and computationally efficient, allowing for very quick computing times and real-time updates. To minimize weight on the UAV, the team decided to run the OAP on the GCS and not add an onboard processor.

2.4. Imaging System

To successfully complete *ODCL*, a high resolution, lightweight camera was needed. Important design points considered when choosing a camera included lens type (mirrorless, mirrored), shutter speed, weight, size, and resolution. The images taken by the camera in the search area must also meet a minimum resolution threshold required by the autonomous image processing system. Through the calculations conducted in **Equation 1** and extensive testing of the autonomous image processing system, this minimum resolution value was computed to be 1.5 Pixels Per Square Inch (PPSI).

Equation 1: Pixels per Square Inch Calculation

$$PPSI = \frac{\text{megapixels} * 1,000,000}{FOV(\text{horizontal}) * FOV(\text{vertical})}$$

After researching numerous options, the team chose the Samsung NX500 due to its high shutter speed, low weight, and high resolution. **Table 4** outlines important statistics for the different cameras considered. Both the Sony A6000 and the Samsung NX500 were purchased and tested with targets at a similar altitude to that flown at competition. This testing showed that the Samsung NX500 was able to focus on the targets better and produce a much clearer image. Further, the larger CMOS sensor on the Samsung NX500 provided a greater resolution and increased the image quality.

During testing, it was observed that without a gimbal, images would suffer extensive motion blur. Preventing the motion blur required the Samsung NX500 camera to be mounted to a 2-axis brushless gimbal. The Arris Zhaoyun 2-Axis Brushless gimbal was chosen because of its SimpleBGC control board which is controllable via the Pixhawk 2.1's auxiliary outputs, enabling the team to maintain both autonomous and manual control over the camera's Field of View.

Table 4: Camera Comparison

Camera	Megapixels	Focal Length (mm)	Test Altitude (feet)	PPSI at Height	Weight (Grams)	Area per Picture (ft^2)
Sony A6000	24.3	20	350	1.44	413.62	117,472.05
Samsung NX500	28.2	20	350	1.5	431.48	101,400.00
GoPro Hero 5 Session	10	32.3	150	.88	60.67	78,993.77

Testing showed that the maximum speed the search area can be completed is 16 knots. The imaging system was tuned for conducting the search area at that speed. To determine the rate at which the camera would take photos, the team first calculated the time it would take the UAV to traverse the area that would be photographed in a single photo from the camera. The team then calculated the necessary overlap between photos to ensure that no targets would be missed and adjusted the first derived time to compensate. These resulting calculations were then tested,

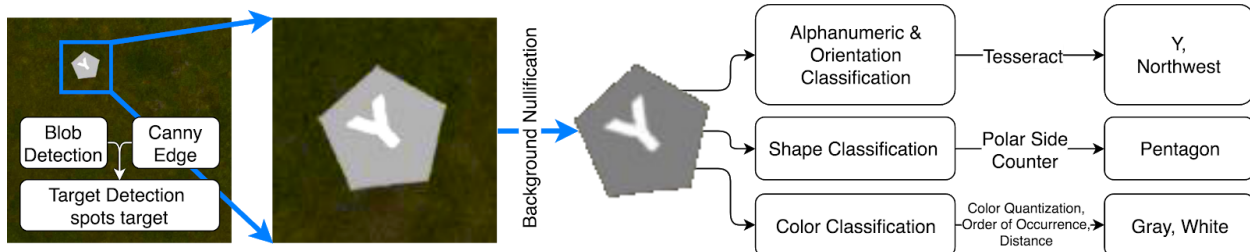
and the results provided the team with high confidence that taking one image every ten seconds would be adequate to complete *Object Detection, Classification, and Localization*.

2.5. Object Detection, Classification, Localization (ODCL)

2.5.1 Design

In order to address the *ODCL* mission task, an open source library was developed to enable both manual and autonomous image processing capabilities. The entire system was rewritten from last year's system to be cleaner, more efficient, and more fine-tuned for Spirit X. **Figure 6** illustrates the process by which autonomous image processing is completed and how each individual component contributes to a successful mission demonstration.

Figure 6: Autonomous image processing breakdown

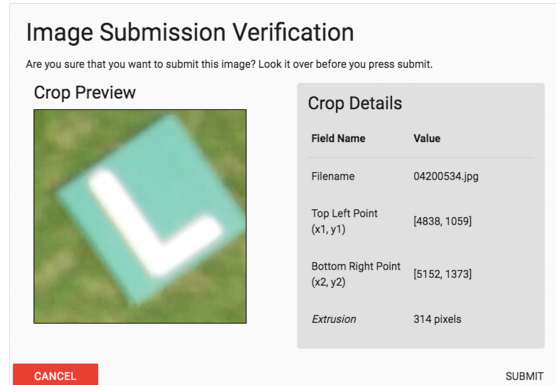


In order to test all image processing systems on a large dataset, the team developed a highly customizable and modular synthetic dataset generator, which simulates the aerial target map images taken by the aircraft at competition. Each synthetic target map is constructed of a background image with a specified number of overlaid targets. The background image is modified from real images taken in previous years at competition and each of the targets is constructed from one of the 13 allowable shapes and an alphanumeric character and assigned colors, proportionalities, and orientations. In addition to constructing full synthetic images, the synthetic dataset generator is able to create simulated crops of single targets. With the ability to create large sets of synthetic target images, all image processing components were able to be extensively unit and simulation tested. To conserve space, the results of all testing conducted on the image processing system are described in Section 2.5.7.

2.5.2 Manual Target Submission

The Manual Target Submission System (MTSS), as shown in **Figure 7**, allows team members at the flight line to manually identify and submit targets simultaneous to the execution of the autonomous image processing system.

Figure 7: Manual Image Submission Platform

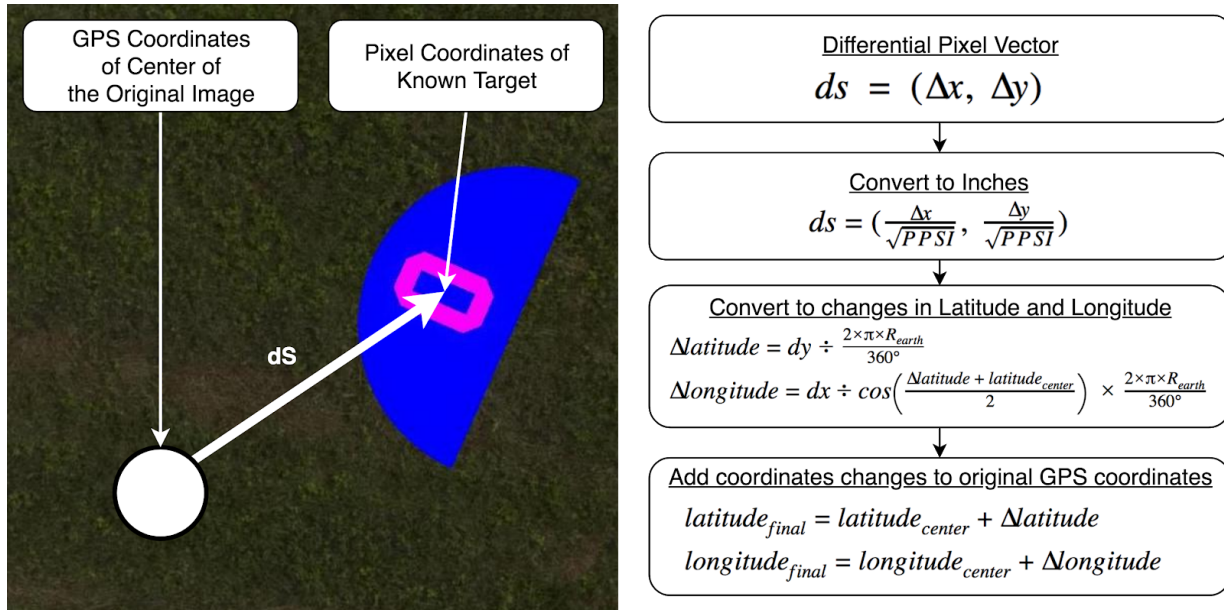


Field Name	Value
Filename	04200534.jpg
Top Left Point (x1, y1)	[4838, 1059]
Bottom Right Point (x2, y2)	[5152, 1373]
Extrusion	314 pixels

Once a target is identified by a user, an automatic localization algorithm determines the target's location by matching the picture snapshot time, determined from the metadata of the image file, with the corresponding time in

Spirit X's location log. During flight, this log is updated at 4 Hz with Spirit X's geolocation. The gimbal ensures that the camera is always directly facing the ground so the geolocation of Spirit X at the image snapshot time will correspond to the center of the image as shown in **Figure 8**. Then, the distance between the image's midpoint and the target is calculated in pixels. This pixel distance is converted to meters using the PPSI value calculated for the predetermined search area altitude. Finally, the inverse haversine equation is applied to calculate the target's geolocation.

Figure 8: Autonomous Geolocation Process



2.5.3 Autonomous Target Detection

The autonomous object detection process relies on two essential algorithms provided by OpenCV: Blob and Contour detections. The former operates by detecting blob-like features in the given target map with the confinement of area, circularity, convexity, and inertia. For the latter algorithm to perform desirably, a canny edge detection algorithm is applied to the image in advance. After testing both Blob and Contour detections on variously modified synthetic target maps (equalizing, solarizing, posterizing, inverting, median filtering, etc.), team Animus Ferus discovered that a color-inverted and posterized (bits equals two) image would produce the best result for the former while a posterized (bits equals two) and gaussian-blurred (kernel size equals three) image would be ideal for the latter. Both algorithms return the locations of the centers and the radii of the suspected targets on the images.

After the two lists of suspected targets from an image are determined by the two algorithms introduced above, they are further trimmed down by a customized false positive elimination process, which includes eliminations of over-repeated colors (the two lists are combined after its completion), oversized targets, overlapping targets, and by surrounding colors. With extensive testing, the team has determined the order of the elimination algorithms mentioned above, and the final testing results are shown in **Table 5**, found on page 12.

With the final list of suspected targets having been produced, each target is cropped out from the target map with 30 pixels of margins on each side and passed to the process of background color nullification. To start the process, the average RGB values of pixels on the rim of each crop is calculated. Then, the algorithm scans through all pixels on the selected crop and sets all pixels within 15% difference from the average rim color to transparent. If no exceptions are found after all pixels are scanned, this crop is added to the list of eliminated crops and the background color nullification process stops for this crop. Otherwise, the algorithm continues to scan the surrounding colors of each pixel, setting it to transparent if three of the four neighboring pixels of the pixel scanned are transparent or if all pixels with distance two away from the pixel scanned are transparent. Finally, the image is re-cropped with 5 pixels of margin on each side of the target. All crops from the target detection and background color nullification processes are passed to the next stage of image processing, and the crops added to the list of elimination are removed as false positives.

2.5.4 Autonomous Color Classification

In order to accurately identify the color of the shape and alphanumeric content, a combination of k-means for color quantization and pixel count statistics were used.

The color classification process begins by using the k-means algorithm to reduce the number of colors in the image to three. After the image's colors are reduced, five horizontal, equidistant pixel rows are taken from the post k-means image and the frequency of each color is determined. The color with the highest occurrence is assumed to be the shape color, and the second highest assumed to be the alphanumeric color. The third, remaining color is assumed to be the remnants of any part of the background that was not fully eliminated in previous target detection operations.

2.5.5 Autonomous Shape Classification

The algorithms that complete autonomous shape classification initially receive potential target crops which have backgrounds set to alpha pixels, as shown in **Figure 9A**. This image is then processed so that only the edges of the image are highlighted. The image generator iterates through all of the pixels in the target crop and determines where the image edges are based on the alpha pixels. This image, shown in **Figure 9B**, is then classified by OpenCV's contouring algorithm, and seven Hu invariants are calculated from this contour. These Hu invariants of the target image are compared with a number of different pre-drawn shape filters. This comparison is quantified by summing the difference between each corresponding Hu invariant. The correct shape is chosen by selecting the shape filter with the least comparison difference. Each possible shape has a number of different filters that vary slightly in shape and orientation, ensuring that the correct shape will be chosen regardless of varied dimensions or orientations. **Table 5** shows the results of testing the system on both synthetic and real targets.

During the development of the shape classification system, a number of different algorithms were tested. Initially, a polar side counter was developed which used raycasting to determine how far each edge pixel is from the midpoint of the image and its corresponding angle. However, this method was not adequate because of the low PPSI, which caused the algorithm to produce inaccurate results. Using contour and shape filters improved the program's accuracy by a factor of four, increasing from 15% to 70% in testing.

2.5.6 Autonomous Letter and Orientation Classification

Both alphanumeric and alphanumeric orientation classifications are based on the Tesseract algorithm. Before initiating these classifications, the background color nullification algorithm from the autonomous target detection system is applied again to the resulting images of Autonomous Target Detection to segment the alphanumeric values from the targets.

To determine the alphanumeric, each resulting image crop goes through the process of 45-degree-rotation and the image-to-string method of Tesseract for eight turns. The result of each turn is recorded and the result with the highest occurrence is determined to be the correct classification.

The letter orientation classification also utilizes the result obtained from the Tesseract algorithm. Since the image crop is rotated 45-degrees for eight times, each rotation would result in a unique cardinal direction. The mean of the cardinal directions with the correct alphanumeric determined above is taken as the correct orientation. Integrating autonomous letter and orientation classification has been an extensive process, and the team did not have time to test the autonomous letter and orientation classification components.

2.5.7 Developmental Testing

Every component of the image processing system has been tested extensively by the team. Tests are conducted on both the customized synthetic dataset and images taken by Spirit X. Testing results for each component are displayed in **Table 5** below.

Table 5: Autonomous Target Detection Testing

Synthetic		Real	
Number of Synthetic Targets	100,080	Number of Real Targets	36
Number of Synthetic Targets Detected	91,496	Number of Real Targets Detected	30
False Positive Count	1,882	False Positive Count	2
Success Rate	91.42%	Success Rate	83.33%
Autonomous Shape Classification			
Number of Shapes Correctly Classified	63,164	Number of Shapes Correctly Classified	23
Success Rate	69.04%	Success Rate	76.67%
Autonomous Color Classification			
Number of Shape Colors Correctly Classified	90,617	Number of Shape Colors Correctly Classified	29
Shape Color Classification Success Rate	99.04%	Shape Color Classification Success Rate	96.67%
Number of Alphanumeric Colors Correctly Classified	57,640	Number of Alphanumeric Colors Correctly Classified	14
Alphanumeric Color Classification Success Rate	63.01%	Alphanumeric Color Classification Success Rate	46.67%

2.6. Communications

Spirit X utilizes multiple wireless links to maintain communication with the GCS. The communication system was designed to provide high-bandwidth connections at distances exceeding 2.5 km, ensuring that Spirit X will not lose connection with the GCS or with the backup safety pilot during the mission demonstration. **Figure 10** shows a block diagram of the communications system and outlines how each component interacts with the system as a whole.

Operating on the 915 MHz frequency band, Spirit X's RFD900x module enables high-speed communication with Mission Planner and all other GCS systems. Two half-wave 3 dBi omnidirectional antennas are mounted to Spirit X in different polarizations to ensure that the UAV does not lose communication with the GCS, regardless of its orientation. A 10 dBi directional patch antenna is located on the ground. Both the RFD900x modules transmit at +30 dBm. The high-powered system provides a reliable, high-bandwidth connection between the GCS and the UAV. The 2.4 GHz frequency band is used as the communication channel for the RC receiver. The RC receiver uses a 3 dBi omnidirectional antenna, with a transmission power of +20 dBm.

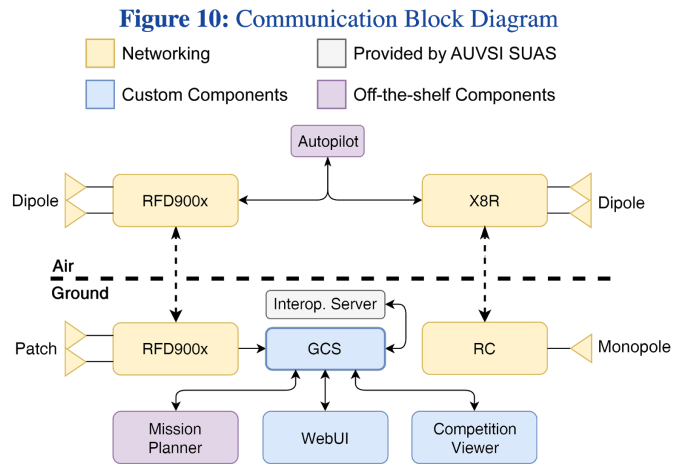


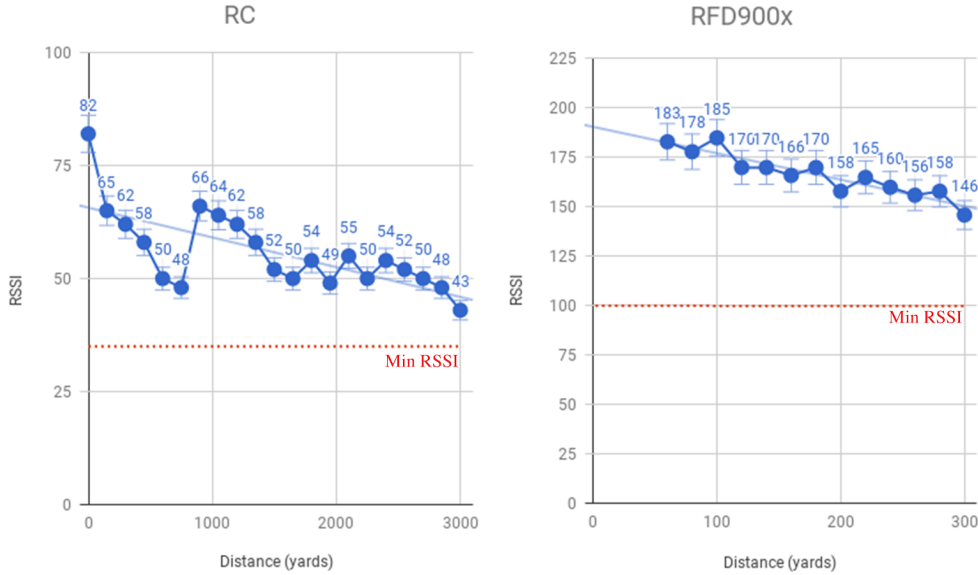
Figure 11: RC Link Testing (left) GCS Link Testing (right)


Figure 11 shows range testing conducted with both the RC and GCS links. The graph on the left of the figure shows the results from the RC link test. As evident in the graph, the link is able to operate nominally at distances of 3000 yards, or roughly two miles. The graph on the right of the figure shows the results of the GCS link test, which was tested 300 yards away from the UAV. These tests verified that the UAV will not lose connection with the Ground Control Station or the Safety Pilot at any point during the mission demonstration.

2.7. Air Delivery

The air delivery mechanism, shown in **Figure 12**, consists of a custom 3D printed cylinder with a metal geared servo mounted on the side. A servo horn, also 3D printed, is then attached to the servo. The arm, when closed, is held underneath a protruding structure that locks the payload in place. When signaled by the autopilot, the servo swings open, releasing the water bottle. The specifications for the air delivery mechanism are outlined in **Table 6**.

Because this year's task requires the payload to open on impact, team Animus Ferus decided that a parachute or similar drag inducing design was not necessary. Eliminating the parachute allowed for a smaller and lighter mechanism that not only reduced weight but also reduced the air resistance that was exerted on the UAV as a result of the mechanism's footprint.

Since Spirit X is a multirotor, it is able to hover directly over the air drop location. This, in combination with the drag reduced design, ensures that the payload is delivered with pinpoint accuracy. Further, this reduces the system complexity since an optimal drop time does not need to be calculated including the UAVs velocity.

Table 6: Air Delivery System Specifications

Weight (without bottle)	Weight (with bottle)	Height	Base Width
83 grams	340 grams	135 mm	99 mm

The air delivery mechanism was tested extensively during development. The servo was tested in multiple simulated air deliveries, which enabled the team to ensure it was strong and wear-resistant. Additionally, because the UAV will be operating in a high temperature environment, potentially exceeding 100 degrees fahrenheit, the 3D

Figure 12: Airdrop Model


printed component was tested to determine the temperature that would cause the plastic to deform. The component was able to withstand temperatures of 131 degrees fahrenheit prior to the occurrence of deformation.

Further testing was conducted to determine the accuracy of the air delivery mechanism. These tests, shown in **Figure 13**, show that the mechanism is able to deliver the payload with an average accuracy of 6 feet. The maximum distance recorded was 11 feet, which occurred during wind gusts.

2.8. Cybersecurity

Ensuring all communications links between the UAV and the GCS are secure is key to protect all involved parties' intellectual property and to ensure everyone's safety. All communication links with Spirit X are protected with frequency hopping and spread spectrum. Further, the RC transmitter is bound to Spirit X, ensuring that other RC transmitters are unable to fake the signal and take control of the UAV. To protect Spirit X's link with the GCS, RFD900x modules implemented AES-128 bit encryption. During testing, the team verified the link was encrypted by unsuccessfully trying to use an unencrypted module to interfere with the communication between the encrypted modules.

In addition to securing the communication links, other potential attack vectors were mitigated. These included GPS spoofing, GPS jamming, and telemetry jamming. **Table 7** outlines these attacks, their impact, and how they were mitigated.

Table 7: Cybersecurity Risks and Mitigations

Component	Risk	Impact	Mitigation
GPS	Spoofing	Erroneous location data	Use of two GPS modules for redundancy. Modules implement protections against these attacks
	Jamming	Loss of location data	
Telemetry	Jamming	Loss of communication	Frequency hopping
	Monitoring	Leak of protected information	AES encryption and frequency hopping
Control link	Man in the middle attack	Unintended actions of vehicle or false telemetry readings	
	Jamming	Loss of communication	Frequency hopping
	Man in the middle attack	Unintended actions of vehicle or false telemetry readings on RC controller	

3. Safety, Risks, and Mitigation

Safety is at the core of all developmental and flight operations that are conducted. A designated Safety Officer (SO) is responsible for ensuring the safety of all team members and all equipment. Numerous safety protocols and procedures were developed to mitigate risks associated with developing and operating a multirotor UAV.

3.1. Developmental Risks & Mitigations

Each team member was trained in the operation of all equipment. Safety is of paramount importance during every test conducted and throughout the entirety of development all necessary safety equipment was on hand. For example, safety glasses, fire extinguishers, and Li-Po safe bags were used appropriately to minimize safety risks posed to team members and equipment. Additionally, the team followed a strict safety protocol and checklist before each test to ensure the safety of both the team and Spirit X. One of the key protocols implemented ensures only one team member, the SO, was allowed to approach the UAV once powered. This ensured that individuals not trained to manage the UAV were ever at risk of being harmed.

3.2. Mission Risks & Mitigations

Table 8, below, outlines the risks Animus Ferus identified and their respective mitigations. These risks encompass those in operational tests, test flights, and the mission demonstration.

To comply with all requirements set forth by AUVSI, in the event that Spirit X loses connection to either the GCS or the backup pilot, the craft will automatically return home, ensuring the persistent connection of the other communications link.

Safety checks are conducted during each step of Spirit X's operation to ensure the greatest possible risk mitigation. Additionally, safety equipment is readily available throughout all flight operations. A preflight briefing is conducted to ensure all team members are aware of safety protocols specific to the flight or operational test.

Numerous safety risks are posed by operating the UAV at competition. In particular, Spirit X's use of Carbon-Fiber propellers presents a significant safety risk to those near the UAV during operation if a malfunction occurs. These risks are mitigated by the strict adherence to preflight checks and safety protocols before, during, and after each flight. To mitigate risks associated with vehicle proximity to the flight line or surrounding objects, the UAV always flies within a geofence.

Table 8: Identified Risks and Mitigation

Risk	Frequency	Impact	Mitigation
Injury to personnel in preflight setup or postflight teardown process	Rare	High	Only trained personnel are allowed to approach the UAV. All personnel practice properly handling malfunctions.
Electrical Failure	Rare	High	Redundant electrical systems for all systems on the UAV.
Damage to Li-Po batteries	Rare	High	Safe transportation, consistent monitoring, and protocols to properly handle disposal of batteries in the event of a crash.
Human Error	Infrequent	Medium	Strict adherence to safety protocols at all times.

4. Conclusion

Team Animus Ferus' hard work and thorough design and testing have led to the final version of Spirit X as described in this Technical Design Paper. Spirit X's in-house design and engineering represents a significant milestone for the team and enabled the UAV to integrate numerous technologically advanced components such as 3D printed parts and an autopilot system. Spirit X's new redesigned electrical, communication, propulsion, airframe, autopilot and flight control systems all provide significantly improved flight characteristics and reliability. Further, the extensive testing conducted by the team verified the integrity of each individual component and its ability to integrate into the final Spirit X UAV. The result of the team's extensive work is a strong competitor for the 2018 AUVSI SUAS competition.